Simple models for penetration of thick targets by rigid projectiles

S. Syngellakis
Wessex Institute of Technology, UK

Abstract

This paper discusses the material characteristics that influence resistance of thick targets to penetration by rigid projectiles and critically reviews simple analytical models for predicting the time history of the impact force and other response variables over a practical range of impact energies. The scope of the reviewed analyses is enhanced by accounting more rigorously for the contact geometries and introducing empirical relations for the parameters adopted in the simplified models. The analyses are implemented through a computer code whose effectiveness and reliability are tested on realistic impact events from the relevant technical literature. Comparisons are also made with finite element results. It is thus shown that the shock loading on a structure and its appendices can be reliably and efficiently predicted by a simple penetration analysis. Various means of enhancing the scope and effectiveness of the model are suggested.

Keywords: impact, projectile, penetration, cavitation, modelling.

1 Introduction

The response of thick, protective plates to high-energy impact varies considerably with the type, range and intensity of attack, as well as plate geometry, material and support conditions. Although the integrity of the plates themselves can be guaranteed by the current design methods, the design trend towards increased resistance to penetration means that a greater proportion of the impact energy would be transmitted to and absorbed by the rest of the protected structure; this development has important implications for the design of the plate attachments. Moreover, the high intensity of the resulting dynamic excitation may adversely affect sensitive equipment within the structure.

www.witpress.com, ISSN 1743-3509 (on-line)
doi:10.2495/SU120061

These design issues can be addressed by adopting a two-stage approach whereby a reliable description of the impact loading is generated first and then used as an input to a global dynamic analysis. The first stage considers the missile-target interaction accounting for the time-dependent, elasto-plastic properties and contact geometries of both colliding bodies. Local and global dynamics can be considered decoupled on the assumption that the duration of impact is significantly shorter than the fundamental period of vibration of the whole structure.

Penetrating projectiles, relying only on their kinetic energy, have been designed in various shapes and sizes for optimum performance. Their material response to impact depends, to a large extent, on their impact velocity, which varies widely in practice. This is taken into account through the development of distinct penetration analyses for rigid and deformable projectiles. Shape charges, undergoing hydrodynamic deformation on impact rely on chemical energy as the source of their penetration power. Their interaction with targets may be analysed by simplified methods similar to those applied to a deformable projectile [1, 2].

The trend towards thicker, perforation-resisting plates has led to the idealisation of thick targets as semi-infinite media and the modelling of their penetration under normal projectile incidence. Thus, the safety of a particular design can be ascertained and the minimum plate thickness for a given impact energy identified. The same numerical process can actually be used iteratively to solve the reverse problem, that is, yield the minimum impact energy required to perforate a plate of given thickness.

A comprehensive analytical solution to the problem of local, non-linear plate deformation under impact, accounting for all observed phenomena, is not available. A direct way of addressing the problem is through test data correlation. This, however, is prohibitively expensive due to the extensive experimentation required for the correlation of the large number of modelling parameters involved [3]. Alternatively, finite element (FE) and finite difference (FD) formulations of continuum theories, rigorously modelling the complex material behaviour, can be applied; such numerical tools have indeed provided valuable and detailed information on impact responses but they have also been found time-consuming and computationally expensive. Simplifying assumptions have allowed the development of fast and economical, semi-empirical analytical tools, appropriate to specific impact events or ranges of parameters. Such simple analyses, based on fundamental physical laws and available experimental evidence, are particularly helpful to the design of impact experiments since they quickly yield estimates of the expected response for various combinations of materials, sizes and geometries. Test measurements are subsequently contributing to the calibration and validation of both the simple as well as rigorous analytical approaches.

The design of structures against impact is often based on the empirical functional relationship

$$\frac{U}{V} = \text{constant} \tag{1}$$

www.witpress.com, ISSN 1743-3509 (on-line)

between the available kinetic energy for impact U and the volume of displaced material V. Eqn (1) has been used in various engineering contexts, from ship collisions [4] to ballistics [2]. It has been the starting point for the derivation of numerous penetration formulae and, in its simplest form, can readily provide first estimates of material density or dimensions of the missile required to penetrate a plate of given thickness [2]. It is not however possible to obtain from it any information about the intensity, variation and duration of the impact force.

This paper reviews, assesses and applies simple penetration theories for rigid projectiles that can readily provide time histories of all important variables describing an impact event. The effectiveness and reliability of these models are improved through the generation of useful empirical relations providing rational estimates of key modelling parameters. The equations of motion are integrated through established numerical schemes suited to the particular type of implemented analysis. The computed results are compared qualitatively and quantitatively with published experimental measurements and analytical predictions.

2 Basic theory and assumptions

The phenomena accompanying penetration into thick targets have been observed to occur in three stages [3]: (a) shock wave propagation, (b) quasi-steady material flow field and (c) either failure of target material resulting in perforation or termination of penetration and rapid transition to projectile rest. The second stage has been found to dominate the deformation process, especially in the case of long, slender projectiles [5]. Its mathematical modelling through a simple theory can provide the pattern and duration of impulse. Normal incidence of an axisymmetric projectile on a semi-infinite medium is assumed as this is expected to cause maximum damage for a given impact energy. The projectile headshape may be described in cylindrical coordinates by a function $r = r(z)$ as shown in fig. 1. In simple analytical models, the expression

$$p = a\sigma_{ft} + b\rho_t \dot{x}^2 \tag{2}$$

has been adopted for the normal pressure p on the target where a dot above a symbol means differentiation of the represented variable with respect to time; σ_f and ρ represent dynamic flow stress and density, respectively, subscript t indicates a target property or variable, x is the projectile penetration, and a, b parameters depending mainly on the material, geometry and speed of the projectile. The frictional component of traction can be introduced into the analysis through the simple model [6]

$$f = \mu p \tag{3}$$

where μ is the coefficient of sliding friction. There is considerable uncertainty about the appropriate value for μ but numerical results do not appear particularly sensitive to its variation. It has been argued that the formation of a thin layer of melted material over the missile-target interface renders friction negligible and thus justifies its omission from simplified [7] or numerical [8] analyses.

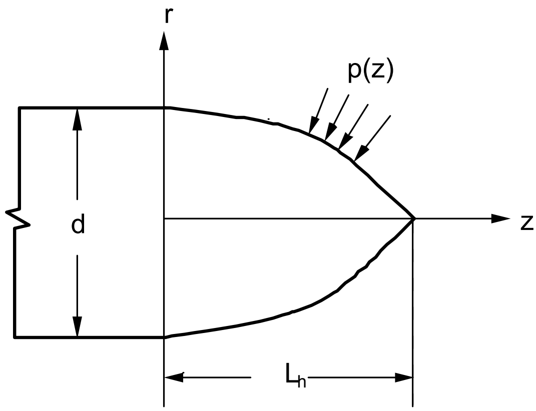

Figure 1: Projectile head geometry.

Parameter a basically accounts for the kinematic constraint on plastic deformation in the neighbourhood of the impact zone. Its value does therefore depend on the geometry of the projectile-target interface and the extent of penetration. The flow stress in eqn (2) is not itself a fixed quantity since plastic strain varies both spatially and with time. In most applications of simplified analyses however, σ_{ft} is assumed constant and, in such a case, a representative value needs to be identified. A simple means of accounting for its dependence on plastic strain is to take it equal to the mean of the target yield stress and tensile strength; it is however expected that it would be closer to the latter value since significant plastic strains develop even under low-energy impacts [9]. It is obvious that the flow stress would be more accurately estimated for materials with low strain hardening.

The dynamic effect on σ_f is reliably assessed through tensile tests performed under various strain rates. Various constitutive models relating flow stress to strain rates have been proposed [9] but their validity has been established only for a few metallic substances. Over the lower strain rate range, a formula attributed to Malvern is often quoted [9]; for rigid-plastic materials, it takes the form [10]

$$\frac{\sigma_f}{\sigma_{f0}} = 1 + \frac{\sigma_Y}{\sigma_{f0}} \left(\frac{\dot{\varepsilon}}{D} \right)^{\frac{1}{m}} \tag{4}$$

where σ_{f0} is the flow stress obtained under quasi-static conditions, σ_Y the nominal yield stress, m is the logarithmic strain rate sensitivity and D a constant. The applicability of eqn (4) has only been tested on mild steel and a particular aluminium alloy over specific strain rate ranges. It has been suggested that the model parameters depend strongly on the magnitude of developing strain rates [11]. This is consistent with the finding that the flow stress shows very little sensitivity to strain rate variations at strain rates above 100 s^{-1} [12]. An empirical linear relation between dynamic flow stress and strain was obtained from a considerable amount of experimental data; the material parameters entering that relation depended only on the Brinnell hardness of the metallic substances tested.

Estimates of the strain rates developing as a consequence of a particular impact event can be deduced from the kinematically admissible fields yielding upper bound solutions to indentation problems [13, 14]. Considering, in particular, the strain rate distribution within centred fans of shear lines, it can be shown that the mean strain rate value can be linked to the projectile velocity by a simple linear relation that involves also the diameter and the headshape of the projectile. It is thus possible to predict with sufficient accuracy the order of magnitude of developing strain rates. Finite element analyses of high speed penetration produced strain rate results consistent with the predictions of such a simple formula [15, 16].

The rate of penetration is equal to the projectile velocity u and the equation of motion of the projectile is

$$m_p \ddot{x} = -F(x, \dot{x}) \tag{5}$$

where m_p is the projectile mass and F the resultant impact force resisting penetration given by

$$F(x, \dot{x}) = 2\pi \int_0^{r_c(x)} p(r, \dot{x}) r \mathrm{d}r \tag{6}$$

in which p is substituted from eqn (2), $r_c(z_c)$ is the radius of the boundary of the contact area and $z_c = L_h - x$, where L_h is the head length. The size of the contact area mainly depends on the impact velocity and the mode of projectile-target interaction; therefore, it needs to be specified for each range of key impact parameters.

3 Low impact velocity

The appropriate value for a, corresponding to a particular headshape, is provided by the solution of the respective quasi-static indentation problem. Upper bound analyses with smooth pyramid indenters [14] have yielded relations between a and the half-apex angle. These values include the effect of material "pile-up" at the faces of the pyramid. For a square flat indenter, both lower and upper bound solutions for the pressure have been obtained [17] pointing to the actual value of a being very close to 3. It is thus reasonable, as Johnson [9] suggested, to adopt the value $a = 3$ in analyses of low velocity impacts with blunt indenters.

As mentioned above, the flow stress is expected to be affected by strain rate for $\dot{\varepsilon} < 100\ \mathrm{s}^{-1}$; σ_f would therefore indirectly depend on penetration velocity. Finally, the second term on the left-hand side of the pressure formula (2) can be considered negligible compared to the first. As a consequence, the target resists penetration by a uniform normal traction

$$p_0 = a\sigma_{ft} \tag{7}$$

applied over the projectile head or that part of it which is instantaneously in contact with the target material. The initial penetration phase is thus dominated by the projectile headshape and velocity. The effect of the latter can be accounted for by adopting an average value for the dynamic flow stress σ_f. Thus p_0 can be considered constant and, by eqn (6), the resisting force is found from

$$F(x) = p_0 \pi \, [r_c(x)]^2 \tag{8}$$

which shows that it depends only on penetration. The time history of projectile velocity is thus obtained by analytical integration of eqn (5). The penetration itself is subsequently calculated using numerical quadrature and substituted back in eqn (8) to yield the impact force. When x exceeds L_h, F becomes constant and the solution of eqn (5) trivial. In the case of a projectile with conical head, the maximum indentation diameter is found equal to

$$d_i = 2\tan\alpha \left(\frac{3 m_p u_0^2}{2 p_0 \pi \tan^2 \alpha} \right)^{\frac{1}{3}} \tag{9}$$

where α is the semi-apex angle and u_0 the impact velocity.

4 High impact velocity

At high impact velocity, the projectile produces a tunnel through the target material and therefore a must reflect this mode of plastic deformation. Various elasto-plastic solutions for the pressure causing spherical or cylindrical cavity expansion have been obtained [13, 18, 19] and quoted extensively in impact penetration analyses. In the numerical applications discussed in this paper, a is evaluated using the formula [13]

$$a = \frac{2}{3}\left[1 + \ln\left(\frac{2E}{3\sigma_f} \right) \right] + \frac{2\pi^2 E_T}{27\sigma_f} \tag{10}$$

for spherical cavity expansion where E is the elastic modulus and E_T the post yield tangent modulus of the target material. Introducing realistic values of material properties in eqn (10) produces estimates of a well within the range a = 4-4.6 suggested by Wright and Frank [3] in their review of deformable projectile analyses as well as Hill's interpretation of experimental data from impacts of rigid projectiles against lead and copper targets [7].

Hill proposed the use of eqn (2) with the parameter b depending on the headshape through the relation [7]

$$b(r) = K \frac{\mathrm{d}}{\mathrm{d}z}\left(r \frac{\mathrm{d}r}{\mathrm{d}z} \right) \tag{11}$$

where the positive constant K is empirically specified for various headshapes. The adoption of eqn (11) was motivated by a formula for the pressure required to enlarge a cylindrical cavity. Hill considered p_0 as a single parameter, also empirically determined through ballistic trials and incorporating the effects of contact geometry, strain hardening and strain rates on the resistance to penetration.

With eqn (11) substituted in eqn (2), the latter represents the non-uniform distribution of normal pressure over a projectile head of arbitrary shape. The condition that this pressure be non-negative provides an expression for the radius r_c of the contact area. A formula for the critical impact velocity u_c such that r_c is equal to the projectile radius can also be deduced. The so called "cavitation velocity" u_c marks the transition to a crater diameter greater than the projectile diameter. With the initial penetration phase neglected, the expression for the force resulting from eqn (6) is

$$F = \pi r_c^2 \left[p_0 + K\rho_t u^2 \left(\left.\frac{\mathrm{d}r}{\mathrm{d}z}\right|_{z_c} \right)^2 \right] \tag{12}$$

hence it is a function of the velocity only. The equation of motion of the projectile can again be integrated in two steps: first analytically to yield the projectile velocity and then by numerical quadrature to yield the total penetration and the force-time profile.

4.1 Ogive heads

An ogive head shape is represented by the equation,

$$r(z) = \sqrt{\eta^2 d^2 - z^2} - (\eta - 0.5)d \tag{13}$$

where d is the projectile diameter and η a constant parameter greater than 0.5. It is easily shown that the head length is given by

$$z(r = 0) = L_h = \sqrt{\eta - 0.25}\,d \tag{14}$$

The condition that $p = 0$ at $r = 0.5d$ yields the cavitation velocity

$$u_c = \sqrt{\frac{2\eta p_0}{K\rho_t}} \tag{15}$$

and that, for impact velocities lower than u_c, the impact force is

$$F = A_p\, p_0 \tag{16}$$

that is, not dependent on the projectile velocity.

In the presence of cavitation ($u > u_c$), the resisting force is determined from

$$F = \lambda^2 A_p\, p_0 \tag{17}$$

where $\lambda(u)$ is the ratio of cavity to projectile diameter given by

$$\lambda^{\frac{2}{3}} = (2\eta)^{\frac{2}{3}} \left(\frac{2\eta u^2}{u_c^2} \right)^{\frac{1}{3}} - (2\eta - 1)^{\frac{2}{3}} \left(\frac{2\eta u^2}{u_c^2} - 1 \right)^{\frac{1}{3}} \tag{18}$$

This was correlated by Hill [7] to experimental evidence to yield estimates for the parameters p_0 and K for particular values of η.

4.2 Spherical heads

The theory for ogival heads may be considered also applicable to the limiting case of $\eta = 0.5$ which corresponds to a hemi-spherical head. The odd consequence of this approach is that, while the pressure is uniform over the head for $u < u_c$, it becomes a concentrated force at the tip for $u > u_c$. Finite element analysis of steady-state penetration by Batra and Wright [8] indicated that the applied pressure is actually non-uniform and this non-uniformity is gradually increasing with increasing penetration velocity. Cavitation is also predicted to start from the bourrelet and spread gradually towards the tip. These results contradict the behaviour anticipated from Hill's theory [7].

Experimental evidence from impacts of projectiles with hemi-spherical heads [6, 20] is consistent with the expectation of no cavitation up to a certain level of impact velocity. Above that transitional value, the hydrodynamic term, which is supposed to cause cavitation, should contribute to the total normal pressure. The pressure dependence on velocity was, in fact, assumed by Forrestal *et al.* [6] in their alternative simple analysis. Based on the penetration measurements from tests with hemi-spherical heads [6], it was possible to deduce a value for $K(\eta=0.5)$ for aluminium. $K(\eta=\infty)$ can be evaluated from a formula relating it to the material elasto-plastic properties [7]. These results were combined with the scant ogive head data supplied by Hill for mild steel and copper as well as additional data by Forrestal *et al*. for aluminium to generate an empirical normalised K-η relation over the whole range of η for use in numerical applications.

4.3 Conical heads

For conical head shapes,

$$\frac{\mathrm{d}r}{\mathrm{d}z} = \tan\alpha \tag{19}$$

so that, provided that the penetration is greater than L_h, b will be given by

$$b = K\tan^2\alpha = \frac{1}{2}C \tag{20}$$

where C can be interpreted as the drag coefficient. It is obvious from eqn (12) that cavitation should be expected at any impact velocity and that the cavity to projectile diameter ratio is given by

$$\lambda = \sqrt{1 + \frac{b\rho_t u^2}{p_0}} \tag{21}$$

A sufficient amount of data from tests on copper and steel targets allowed the generation of a smooth variation of coefficient K with the semi-apex angle of the conical head [7]; an empirical formula for a normalised K was obtained by polynomial curve fitting through these experimental points.

5 Numerical results

A FORTRAN program was developed to implement both the low-speed and high-speed penetration analyses. The criterion for using the low speed indentation option is that the indentation diameter predicted by the model for each head type does not exceed the projectile diameter. The validity of the code was tested through its application to realistic impact events and comparisons of its predictions with published experimental and analytical results.

5.1 Projectiles with ogive head – no cavitation

A published account of ballistic experiments against thick aluminium targets [21] provided the data for this application of the program. The actual numerical input was: $\eta = 3$, $m = 24.8$ g, $d = 7.11$ mm, $\rho_t = 2710$ kg/m^3, $E = 73.1$ GPa, $\sigma_{ft} = 600$ MPa and $E_T = 150$ MPa. The program was run for three impact velocities and gave the impact force and penetration variations shown in fig. 2. The assumption of rigid projectile and the prediction of no cavitation both conform to experimental observation. The predicted maximum penetrations were in close agreement with the respective experimental measurements and the analytical results obtained through an alternative penetration model that accounts for friction [21]. It seems however that the effect of friction was, in this case, very small and the discrepancy between experimental and analytical results could be attributed to not accounting properly for the strain rate effect.

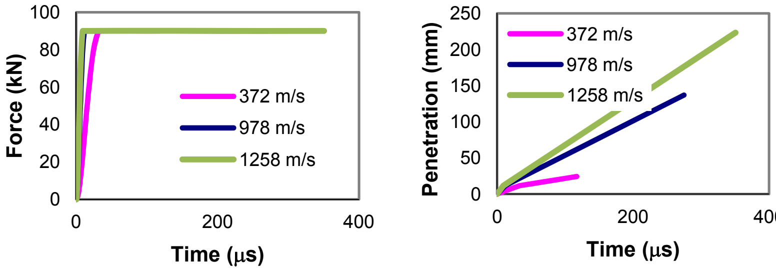

Figure 2: Force and penetration time history for impact without cavitation.

5.2 Projectiles with ogive head - cavitation

The force and penetration time histories shown in fig. 3 were obtained using the data from a test involving steel projectiles against copper targets [7]. The numerical input was: $u_0 = 1$ km/s, $m_p = 10$ g, $d = 7.695$ mm, $\rho_t = 9$ Mg/m^3, $\sigma_{ft} = 346$ MPa and $E = 121.5$ GPa. The generated values for p_0, K, u_c and λ were in reasonably good agreement with the respective published values. The condition $u_0 > u_c$ was satisfied; the cavitation observed in tests was therefore predicted.

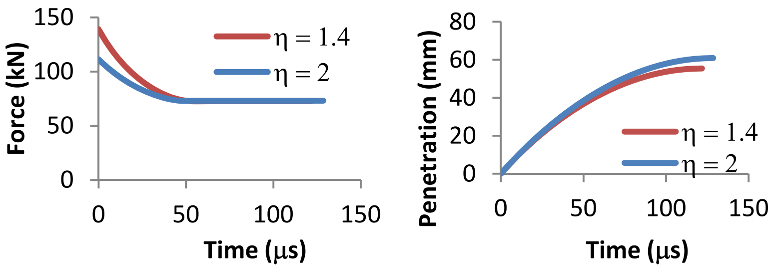

Figure 3: Impact force and penetration with cavitation.

5.3 Projectiles with conical head

The published data from impact tests with steel projectiles against aluminium targets were [6]: $\alpha = 18.4°$, mean $m_p = 23.8$ g, $d_p = 7.1$ mm, $\rho_t = 2.71$ Mg/m^3. The target flow stress, Young's modulus and tangent modulus were taken equal to 400 MPa, 68.9 GPa and 540 MPa, respectively. The impact velocity ranged from 510 m/s to 1370 m/s. The predicted maximum penetration is plotted versus the impact velocity in fig. 4; its agreement with the respective test measurements [6] can be considered satisfactory.

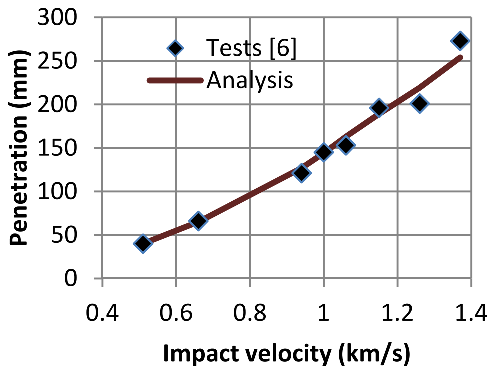

Figure 4: Penetration vs. impact velocity for conical projectile heads.

6 Discussion

The work reported in this paper met its main objective, namely, to re-assess a simple rigid projectile penetration theory in the light of additional experimental evidence and analytical results and to implement it numerically generating time history output that could be useful to structural design against impact. It was thus made clear that the characteristics of the shock loading depend not only on the impact energy but also on the geometry and material properties of the impacting bodies.

A versatile numerical algorithm was developed for the integration of the equations of motion and the generation of shock time histories for a range of projectile head geometries and impact energies. The resulting computer code was extensively applied to impact events described in the literature. Initially, this contributed to the calibration of the various key parameters entering the simple model. Empirical formulae linking these parameters to a geometrical feature of either ogival or conical projectile head were generated and introduced into the FORTRAN code. Subsequent predictions of the program were found in good agreement with other published analytical or experimental results. There is scope for further testing the developed code on the multitude of published impact cases ensuring however that the properties of used materials are specified with adequate accuracy.

The analysis could be enhanced to account for additional types of projectile heads and to represent more effectively the wide range of material behaviour. With regard to projectiles with hemi-spherical heads, the present pressure model needs to be modified so that this special case is addressed with sufficient mathematical rigour and the predicted projectile behaviour is consistent with experimental evidence and finite element solutions.

Particular reference can be made to the need for incorporating the strain rate effect in the analysis. This is conceptually possible at this stage, but the strain rate dependence on projectile velocity means that a numerical step-by-step integration of the equations of motion would be required in all cases. The scheme would require strain rate sensitivity models for various target materials; further literature search but also experimental investigations need to be conducted on this topic.

The modelling can be enriched by the introduction of additional material and geometric parameters and by increasing the confidence in the validity of generated empirical relations. The expansion of the simple penetration model to include the other two stages of penetration and, in particular, the prediction of elastic recovery and bulge forming may be attempted. The model could also be slightly modified to yield rational results for oblique impacts within a limited range of angles of incidence. Progress in modelling can be assisted by referring to the output of relevant numerical work based on advanced constitutive theories. It is however important to try to improve the effectiveness and enhance the scope of the presented theory without substantially increasing its complexity.

The target material in most engineering applications is considered homogeneous and isotropic but recent designs have introduced more effective combinations of metals. Composite, stratified plates with the capacity of resisting high-energy impacts have generated considerable interest among researchers. The simple penetration theory could be developed further to account for the additional complexity and diversity of the problem and thus predict the performance of such targets.

References

[1] Backman, M.E. & Goldsmith, W., The mechanics of penetration of projectiles into targets. *International Journal of Engineering Science*, **16(1)**, pp. 1-99, 1978.

[2] Weihrauch, G., Armour v. KE rounds. *Military Technology*, **(1)**, pp. 23-36, 1987.

[3] Wright, T.W. & Frank, K., Approaches to penetration problems. *Impact: Effects of Fast Transient Loadings*, A. A. Balkema: Rotterdam, pp. 85-103, 1988.

[4] Minorsky, V.U., An analysis of ship collisions with reference to protection of nuclear power plants. *Journal of Ship Research*, **3(2)**, pp. 1-4, 1959.

[5] Christman, D.R. & Gehring, J.W., Analysis of high-velocity projectile penetration mechanics. *Journal of Applied Physics*, **37(4)**, pp. 1579-1587, 1966.

www.witpress.com, ISSN 1743-3509 (on-line)

[6] Forrestal, M.J., Okajima, K. & Luk, V.K., Penetration of 6061-T651 aluminium targets with rigid long rods. *Journal of Applied Mechanics, Transactions of the ASME*, **55(4)**, pp. 755-760, 1988.
[7] Hill, R., Cavitation and the influence of headshape in attack of thick targets by non-deforming projectiles. *Journal of the Mechanics and Physics of Solids*, **28(5-6)**, pp. 249-263, 1980.
[8] Batra, R.C. & Wright, T.W., Steady state penetration of rigid perfectly plastic targets. *International Journal of Engineering Science*, **24(1)**, pp. 41-54, 1986.
[9] Johnson, W., *Impact Strength of Materials*, Edward Arnold: London, 1972.
[10] Symonds, P.S., Viscoplastic behavior in response of structures to dynamic loading. *Behaviour of materials under dynamic loading*, ed. N.J. Huffington, ASME: pp. 106-124, 1965.
[11] Klepaczko, J.R., A general approach to rate sensitivity and constitutive modelling of FCC and BCC metals. *Impact: Effects of Fast Transient Loadings*, A. A. Balkema: Rotterdam, pp. 3-35, 1988.
[12] Recht, R.F., Taylor ballistic modelling applied to deformation and mass loss determinations. *International Journal of Engineering Science*, **16(11)**, pp. 809-827, 1978.
[13] Hill, R., *The Mathematical Theory of Plasticity*, Oxford University Press: Oxford, 1950.
[14] Haddow, J.B. & Johnson, W., Indenting with pyramids-I. Theory. *International Journal of Mechanical Sciences*, **3(4)**, pp. 229-238, 1961.
[15] Batra, R.C., Steady state penetration of viscoplastic targets. *International Journal of Engineering Science*, **25(9)**, pp. 1131-1141, 1987.
[16] Lin, P.-R. & Batra, R.C., Histories of the stress, strain-rate, temperature and spin in steady state penetration problems. *International Journal of Engineering Science*, **27(10)**, pp. 1155-1165, 1989.
[17] Johnson, W. & Mellor, P.B., *Engineering Plasticity*, Ellis Horwood: Chichester, 1983.
[18] Hanagud, S. & Ross, B., Large deformation, deep penetration theory for a compressible strain-hardening target material. *AIAA Journal*, **9(5)**, pp. 905-911, 1971.
[19] Tate, A., Long rod penetration models—Part I. A flow field model for high speed long rod penetration *International Journal of Mechanical Sciences*, **28(8)**, pp. 535-548, 1986.
[20] Forrestal, M.J., Brar, N.S. & Luk, V.K., Penetration of strain-hardening targets with rigid spherical-nose rods. *Journal of Applied Mechanics, Transactions of the ASME*, **58(1)**, pp. 7-10, 1991.
[21] Forrestal, M.J., Luk, V.K., Rosenberg, Z. & Brar, N.S., Penetration of 7075-T651 aluminium targets with ogival-nose rods. *International Journal of Solids and Structures*, **29(14-15)**, pp. 1729-1736, 1992.

www.witpress.com, ISSN 1743-3509 (on-line)